DESY-08-057

# Angular correlations in multi-jet final states from $k_\perp$-dependent parton showers

F. Hautmann[1] and H. Jung[2]

[1] *Theoretical Physics Department, University of Oxford, Oxford OX1 3NP*
[2] *Deutsches Elektronen Synchrotron, D-22603 Hamburg*

## Abstract

Angular correlations in final states with multiple hadronic jets have recently been measured in DIS production at HERA. Next-to-leading-order QCD results for these observables turn out to be affected by sizeable theoretical uncertainties in the kinematic region of the data. We investigate the effects of multiple QCD radiation at higher order using parton-shower methods based on transverse-momentum dependent parton distributions and matrix elements. We observe that significant contributions to the angular correlations measured in three-jet production arise from regions in which transverse momenta in the initial-state shower are not ordered. We present Monte Carlo results for azimuthal two-jet and three-jet distributions, for jet multiplicities and for correlations in the transverse-momentum imbalance between the leading jets. We discuss the comparison with experimental data.

## I. INTRODUCTION

Hadronic final states containing multiple jets have been investigated at the HERA and Tevatron colliders, and will play a central role in the Large Hadron Collider (LHC) physics program. The interpretation of experimental data for such final states relies both on perturbative multi-jet calculations (see [1] for a recent overview) and on realistic event simulation by parton-shower Monte Carlo generators (see e.g. [2, 3]).

Owing to the complex kinematics involving multiple hard scales and the large phase space opening up at very high energies, multi-jet events are potentially sensitive to effects of QCD initial-state radiation that depend on the finite transverse-momentum tail of partonic matrix elements and distributions [3, 4]. In perturbative multi-jet calculations truncated to fixed order in $\alpha_s$ [1], finite-$k_\perp$contributions are taken into account partially, order-by-order, through higher-loop corrections. This is generally sufficient for inclusive jet cross sections, but likely not for more exclusive final-state observables.

On the other hand, standard shower Monte Carlos reconstructing exclusive events, such as Herwig [5] and Pythia [6], are based on collinear evolution of the initial-state jet. Finite-$k_\perp$contributions are not included, but rather correspond to corrections [7–9] to the angular or transverse-momentum ordering implemented in the parton-branching algorithms. The theoretical framework to take these corrections into account is based on using initial-state distributions unintegrated in both longitudinal and transverse momenta [9], coupled to hard matrix elements suitably defined off mass shell. See e.g. [10] for discussion of the Monte Carlo shower implementation of the method. Event generators based on $k_\perp$-dependent showers of this kind include [11–14]. These generators are not as developed as standard Monte Carlos like Herwig and Pythia. However, they have the potential advantage of a more accurate treatment of the space-like parton shower at high energy.

This paper examines the role of initial-state radiative effects in the study of angular correlations and momentum correlations for multi-jet processes. We concentrate on the case of two-jet and three-jet DIS production, for which new experimental results from HERA have recently appeared [15] and next-to-leading-order (NLO) calculations are available [16]. While inclusive jet cross sections are reliably predicted by NLO perturbation theory, jet correlations are found to be affected by significant higher-order corrections, increasing as the momentum fraction $x$ decreases, giving large theoretical uncertainties at NLO. By analyzing angular jet correlations by the $k_\perp$-shower Monte Carlo event generator Cascade [11] and by Herwig [5], we find that sizeable corrections in the kinematic range of the data arise from regions [4] with three well-separated hard jets in which the partonic lines along the decay chain in the initial state are not ordered in transverse momentum. We present Monte Carlo results for azimuthal correlations and transverse-momentum correlations.

The $k_\perp$-shower results describe well the shape of the distributions observed experimentally, and give quite distinctive features of the associated jet distributions compared to standard showers such as Herwig. The largest differences between the two parton showers occur when the azimuthal separations between the leading jets are small, whereas the results become similar when there are two jets nearly back to back. We observe that in the region of small azimuthal distances the largest variation occurs between order-$\alpha_s^2$ and order-$\alpha_s^3$ results in the fixed-order NLO calculations [15, 16], particularly for small $x$. In the region where corrections are not large, the NLO and $k_\perp$-shower results are rather close. Both the $k_\perp$-shower and NLO calculations support a physical picture of multi-jet correlations in which sizeable radiative corrections arise not only from collinear/soft emission, included in Her-

WIG as well, but also from finite-angle emission, associated with the growth of transverse momenta transmitted along the space-like jet.

The above observations suggest the usefulness of combining NLO and $k_\perp$-shower for a broad range of multi-jet observables, in order to obtain more reliable predictions over a wider kinematic region. Monte Carlo results depend on the maximum angle parameter $\mu$ [7, 10, 11] at which the shower is evaluated. The perturbative matching will involve this angle. Studies of the dependence of Monte Carlo results on $\mu$ will be reported elsewhere.

The parton distributions at fixed transverse momentum used in this paper are defined via high-energy factorization [9]. This relates off-shell matrix elements with physical cross sections for $x \ll 1$. Using the dominance of single gluon polarization, it gives a well-prescribed method to introduce unintegrated parton distributions gauge-invariantly in the high-energy region, despite the gluon being off shell. On the other hand, general definitions of $k_\perp$distributions, valid over the whole phase space, are now actively investigated, including the treatment of endpoint divergences [17, 18] and of possible high-order effects from Coulomb/radiative mixing terms [19, 20]. (See e.g. [21, 22], and references therein, for recent studies of pdf operator definitions.) These questions will be relevant for $k_\perp$-shower Monte Carlo generators and for constructing shower algorithms at subleading level, see for instance [23, 24]. In this paper we do not address these issues. More discussion of this and of current limitations in Monte Carlo simulations is given in [4, 25].

Part of the results of this paper have been presented in shorter form in [26].

The paper is structured as follows. We begin in Sec. II by discussing angular correlations in jet final states measured in DIS and corresponding NLO results. In Sec. III we compute jet correlations from parton showering based on unintegrated pdfs and transverse-momentum dependent matrix elements (ME), and compare the results with HERWIG. We consider correlations in the azimuthal angle between the two hardest jets and analyze the distribution of the third jet. We investigate in particular the quantitative effect of the finite high-$k_\perp$tail in the hard ME. In Sec. IV we present results for jet multiplicity distributions and for momentum correlations. We give conclusions in Sec. V.

## II. DIS MULTI-JET FINAL STATES

In this section we recall the experimental results [15] on small-$x$ multi-jet final states. The main focus of the discussion is on jet correlations and potential sources of large QCD corrections.

In Ref. [15] the ZEUS collaboration have presented measurements for two-jet and three-jet production associated with

$$Q^2 > 10 \text{ GeV}^2 \quad , \qquad 10^{-4} < x < 10^{-2} \quad , \tag{1}$$

and performed a comparison with next-to-leading-order calculations [16]. ZEUS measured differential distributions as functions of jet transverse energy and pseudorapidity as well as correlations in azimuthal angles and transverse momenta. The selection cuts on the jet phase space are given by

$$E_{T,HCM}^{\text{jet}-1} > 7 \text{ GeV} \quad , \qquad E_{T,HCM}^{\text{jet}-2,3} > 5 \text{ GeV} \quad , \qquad -1 < \eta_{lab} < 2.5 \quad , \tag{2}$$

where $E_{T,HCM}$ are the jet transverse energies in the hadronic center-of-mass frame, and $\eta_{lab}$ are the jet pseudorapidities in the laboratory frame. The overall agreement of data with

NLO results is within errors [15]. However, while inclusive jet rates are reliably predicted by NLO perturbation theory, jet correlations turn out to be affected by large theoretical uncertainties at NLO. Results from [15] for di-jet distributions are reproduced in Fig. 1 for easier reference.

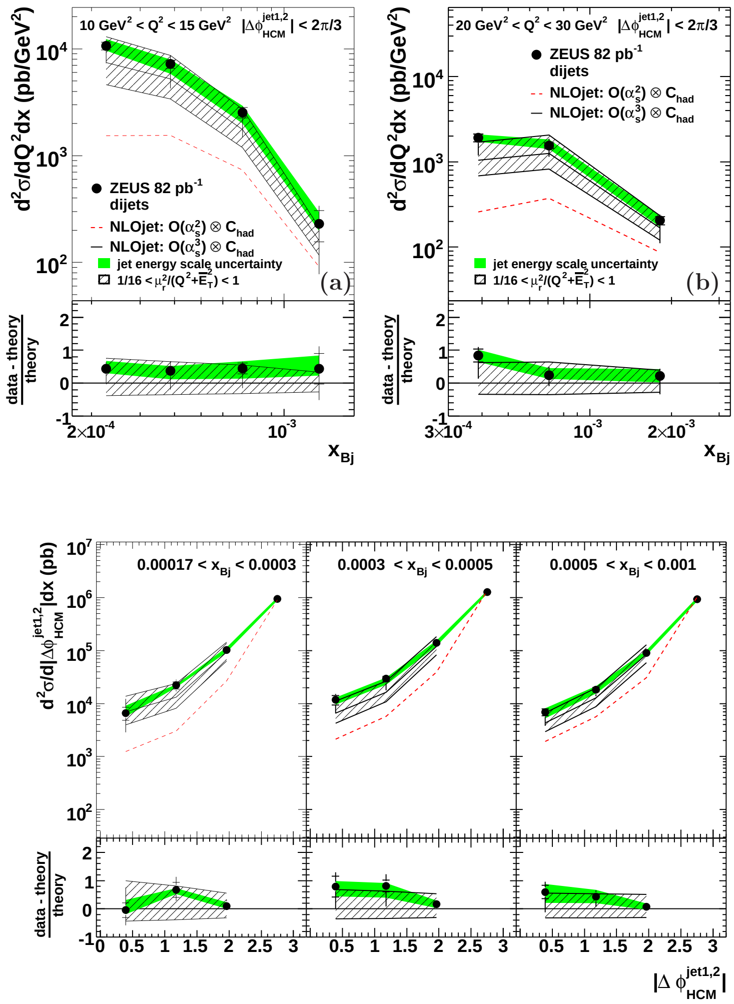


FIG. 1: (top) Bjorken-x dependence and (bottom) azimuth dependence of di-jet distributions at HERA as measured by ZEUS [15].

The plot at the top in Fig. 1 shows the $x$-dependence of the di-jet distribution integrated over $\Delta\phi < 2\pi/3$, where $\Delta\phi$ is the azimuthal separation between the two high-$E_T$ jets. The plot at the bottom shows the di-jet distribution in $\Delta\phi$ for different bins of $x$. We see that the variation of the predictions from order-$\alpha_s^2$ to order-$\alpha_s^3$ is significant. In the azimuthal correlation for a given $x$ bin, the variation increases with decreasing $\Delta\phi$. In the distribution integrated over $\Delta\phi$, the variation increases with decreasing $x$. The lowest order, where the differential cross section $d\sigma/d\Delta\phi$ is non-trivial, is $\mathcal{O}(\alpha_s^2)$ and the NLO calculation is labeled with $\mathcal{O}(\alpha_s^3)$.

Given the large difference between order-$\alpha_s^2$ and order-$\alpha_s^3$ results, it seems to be questionable to estimate the theoretical uncertainty at NLO from the conventional method of varying the renormalization/factorization scale.

Besides angular distributions, a behavior similar to that described above is also found in [15] for other associated distributions such as momentum correlations.[1] We will come back to this in Sec. IV.

The stability of predictions for the jet observables under consideration depends on a number of physical effects. Part of these concern the jet reconstruction and hadronization. The ZEUS [15] and H1 [27, 28] jet algorithm has moderate hadronization corrections [29] and is free of nonglobal single-logarithmic components [30]. The kinematic cuts [15] on the hardest jet transverse momenta are set to be asymmetric, so as to avoid double-logarithmic contributions in the minimum $p_T$ [31]. Note that $Q^2 > 10$ GeV$^2$ (Eq. (1)), and nonperturbative corrections affecting the jet distributions at the level of inverse powers of $Q$ are expected to be moderate.

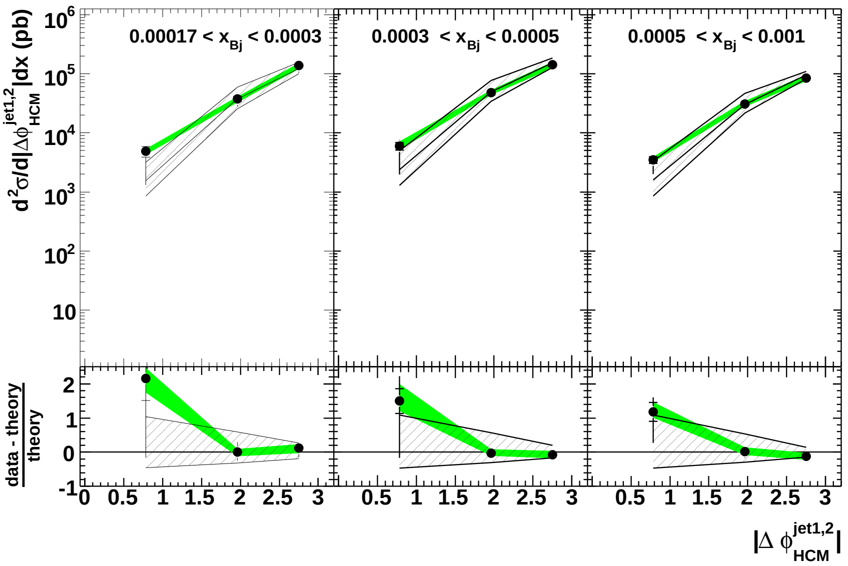


FIG. 2: Three-jet cross section versus azimuthal separation between the two highest-$E_T$ jets as measured by ZEUS [15].

Further effects concern radiative corrections at higher order. Fixed-order calculations beyond NLO are not within present reach for multi-jet processes in *ep* and *pp* collisions. Resummed calculations of higher-order logarithmic contributions from multiple infrared emissions are performed with next-to-leading accuracy in [32]. These contributions are enhanced in the region where the two high-$E_T$ jets are nearly back-to-back. Multiple infrared emissions are also taken into account by parton-branching methods in shower Monte Carlos such as Herwig [5]. Note however that important corrections in Fig. 1 arise for decreasing $\Delta\phi$, where the two jets are not close to back-to-back and one has effectively three well-separated hard jets [4]. The corrections increase as $x$ decreases. Effects analogous to those in Fig. 1 are seen in the ZEUS results for the three-jet cross section, shown in Fig. 2 [15], particularly for the small-$\Delta\phi$ and small-$x$ bins.[2] In Sec. III we analyze the angular distribution of the

[1] On the other hand, NLO results are much more stable in the case of inclusive jet cross sections [15].

[2] The error band for the theory curves in Fig. 2 [15] is obtained by varying the value of the renormalization scale from $(Q^2 + \overline{E}_T^2)$ to $(Q^2 + \overline{E}_T^2)/16$, where $\overline{E}_T$ is the average $E_T$ of the three hardest jets in each event.

third jet, and find significant contributions from regions of the space-like shower where the transverse momenta in the initial-state decay chain are not ordered. These contributions are not fully taken into account either by fixed-order calculations truncated to NLO or by parton showers implementing collinear ordering such as HERWIG and PYTHIA.

In the next section we present the results of computing jets' angular correlations by parton-shower methods that include finite-$k_\perp$corrections to collinear ordering, and we compare these results with HERWIG.

## III. ANGULAR CORRELATIONS FROM $K_\perp$ SHOWER MONTE CARLO

Corrections to the collinear ordering in the space-like shower can be incorporated in Monte Carlo event generators by implementing transverse-momentum dependent parton distributions (unintegrated pdfs) and matrix elements (ME) through high-energy factorization [9]. This method allows parton distributions at fixed $k_\perp$to be defined gauge-invariantly for small $x$.[3] Basic aspects of the parton-shower implementation of the method are discussed in [10]. Monte Carlo generators based on the high-energy definition of unintegrated pdfs (u-pdfs) [9] are developed in [7, 11, 12]. For the calculations that follow we use the Monte Carlo implementation CASCADE [11].

The hard ME in CASCADE are obtained by perturbative computation, while the u-pdfs are determined from fits to experimental data. The parton-branching equation used for the unintegrated gluon distribution $\mathcal{A}$ is schematically of the form [7, 11, 33]

$$\begin{aligned} \mathcal{A}(x, k_\perp, \mu) \; &= \; \mathcal{A}_0(x, k_\perp, \mu) + \int \frac{dz}{z} \int \frac{dq^2}{q^2} \; \Theta(\mu - zq) \\ &\times \; \Delta(\mu, zq) \; \mathcal{P}(z, q, k_\perp) \; \mathcal{A}(\frac{x}{z}, k_\perp + (1-z)q, q) \quad . \end{aligned} \tag{3}$$

The integral term in the right hand side of Eq. (3) gives the $k_\perp$-dependent branchings in terms of the Sudakov form factor $\Delta$ and unintegrated splitting function $\mathcal{P}$. The explicit

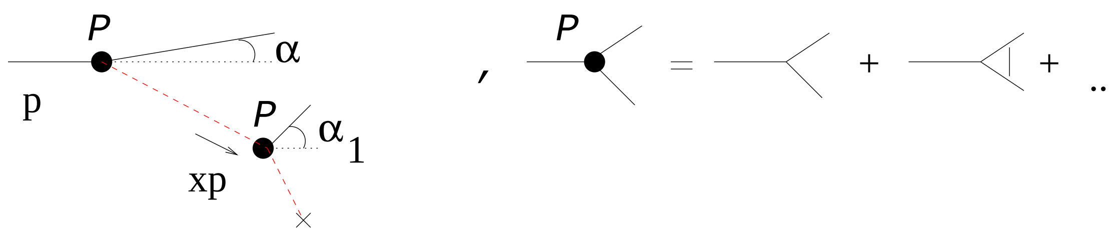


FIG. 3: (left) Coherent radiation in the space-like parton shower for $x \ll 1$; (right) the unintegrated splitting function $\mathcal{P}$, including small-$x$ virtual corrections.

expressions for these factors are specified in [33], and include the effects of coherent gluon radiation not only at large $x$ (as e.g. in HERWIG) but also at small $x$ [8] in the angular region (Fig. 3)

$$\alpha / x > \alpha_1 > \alpha \quad , \tag{4}$$

[3] Operator definitions aimed at extending u-pdfs to the whole phase space, including regularization for the $x \to 1$ endpoint, are studied e.g. in [17, 18] and references therein.

where the angles $\alpha$ for the partons radiated from the initial-state shower are taken with respect to the initial beam jet direction, and increase with increasing off-shellness.

The first term in the right hand side of Eq. (3) is the contribution of the non-resolvable branchings between starting scale $Q_0$ and evolution scale $\mu$, and is given by

$$\mathcal{A}_0(x, k_\perp, \mu) = \mathcal{A}_0(x, k_\perp, Q_0)\ \Delta(\mu, Q_0) \quad . \tag{5}$$

The starting distribution $\mathcal{A}_0(x, k_\perp, Q_0)$ at scale $Q_0$ is parameterized as

$$x\mathcal{A}_0(x, k_\perp, Q_0) = A\ x^{-B}\ (1-x)^C\ \exp\left[-(k_\perp - \lambda)^2/\nu^2\right] \quad , \tag{6}$$

with the values of the parameters $A$, $B$, $C$, $\lambda$ and $\nu$ in Eq. (6) to be determined from data fits. Details on these fits are given in [33, 34]. In the calculations that follow we use the

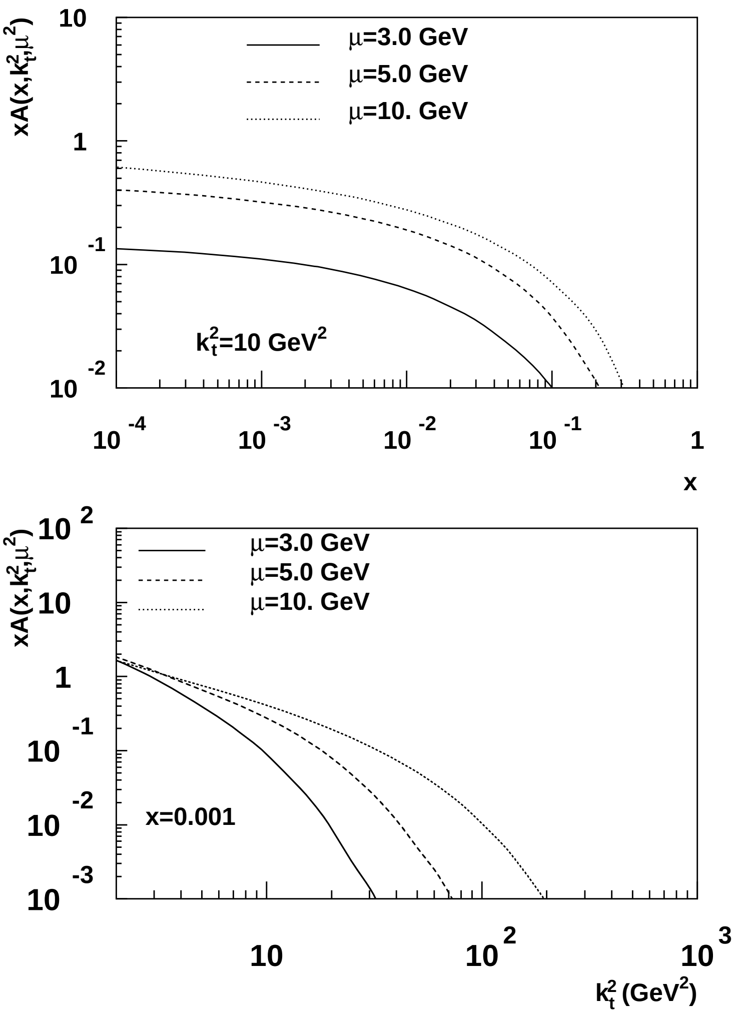


FIG. 4: (top) $x$-dependence and (bottom) $k_\perp$-dependence of the unintegrated gluon distribution at different values of the evolution scale $\mu$.

u-pdf set specified by the following parameter values:

$$\begin{aligned} Q_0 &= 1.1 \text{ GeV} \quad , \qquad A = 0.4695 \quad , \qquad B = 0.025 \quad , \\ C &= 4.0 \quad , \qquad \lambda = 1.5 \text{ GeV} \quad , \qquad \nu = (1.5/\sqrt{2}) \text{ GeV} \quad . \end{aligned} \tag{7}$$

Fig. 4 shows the $x$-dependence and $k_\perp$-dependence of the resulting gluon distribution at different values of the evolution scale $\mu$.

The $k_\perp$-dependent ME and parton branching in Eqs. (3)-(6) lead to a different angular pattern of initial-state gluon radiation than standard, collinear-based showers, e.g. HERWIG. In particular, while the HERWIG angular ordering reduces to ordering in transverse momenta for $x \to 0$ , the $k_\perp$-dependent shower contains finite-angle corrections in this limit [10]. We now compute angular distributions for the DIS three-jet cross section by CASCADE and HERWIG. Let $\Delta\phi$ be the azimuthal separation between the two jets with the highest transverse energy $E_T$,

$$\Delta\phi = \phi_{\rm jet-1} - \phi_{\rm jet-2} \ , \tag{8}$$

where the azimuthal angle $\phi$ for each jet is defined in the hadronic center-of-mass frame. Similarly, we define $\Delta\phi_{13}$ as the azimuthal separation between the hardest and the third jet.

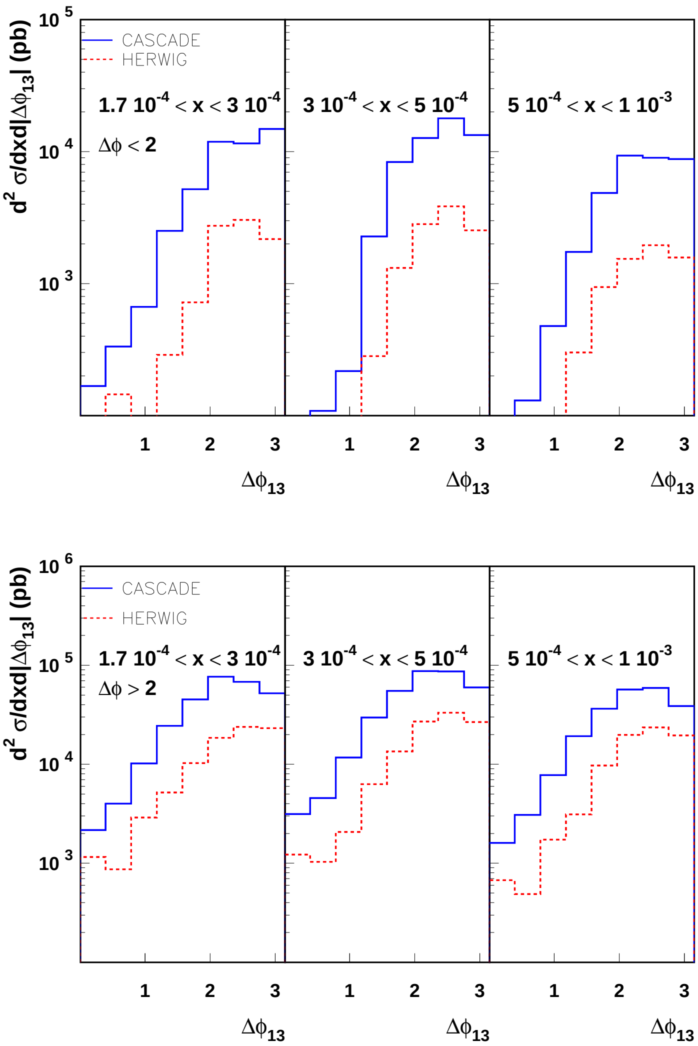


FIG. 5: Cross section in the azimuthal angle $\Delta\phi_{13}$ between the hardest and the 3rd jet for small ($\Delta\phi < 2$, top) and large ($\Delta\phi > 2$, bottom) azimuthal separations between the leading jets. The $k_\perp$Monte Carlo results CASCADE are compared with HERWIG.

In Fig. 5 we compute the three-jet cross section and plot it versus the azimuthal angle $\Delta\phi_{13}$, by distinguishing the cases in which the two leading jets are at small angular separation

($\Delta\phi < 2$) or large angular separation ($\Delta\phi > 2$). Cascade gives large differences from Herwig in the region where the azimuthal separations $\Delta\phi$ between the leading jets are small, see top plot of Fig. 5. This reflects the fact that at small $\Delta\phi$ the phase space opens up for events in which the partonic lines along the initial decay chain are not ordered in transverse momentum. Such configurations are taken into account in Cascade with the appropriate matrix element, at least for small enough $x$, but not in Herwig. The $x$ values considered in Fig. 5 are those corresponding to the three-jet measurements in [15]. As $\Delta\phi$ increases, the results from Cascade and Herwig become closer. See bottom plot of Fig. 5. This is associated with the fact that for $\Delta\phi$ approaching the back-to-back region the phase space for finite-$k_\perp$emissions is reduced. In this region one thus expects both Monte Carlos to give reasonable approximations.

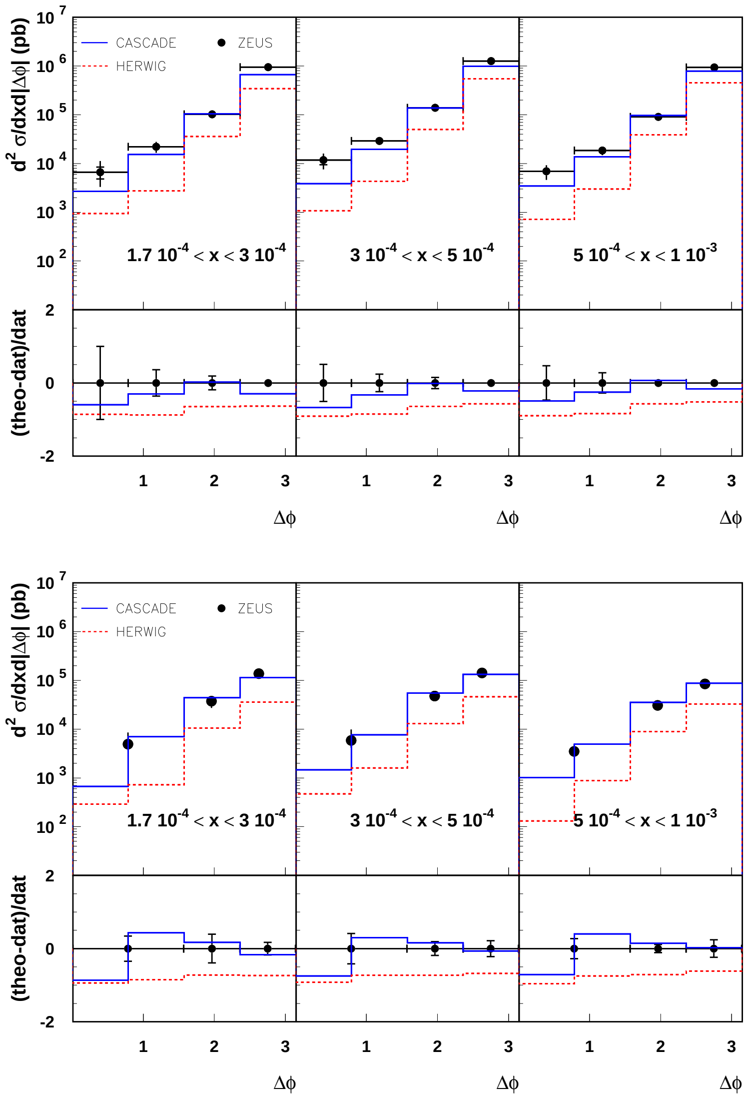


FIG. 6: Angular jet correlations obtained by Cascade and Herwig, compared with ZEUS data [15]: (top) di-jet cross section; (bottom) three-jet cross section.

Fig. 6 shows the angular correlations for DIS final states with two jets and three jets. We compute the azimuthal distribution of di-jet and three-jet cross sections in the separation $\Delta\phi$ between the leading jets. We show the distributions obtained by Cascade and by Herwig, compared with the measurement [15]. Observe that the shape of the distribution is different for the two Monte Carlos. As expected from the result of Fig. 5, CASCADE gives the largest differences to HERWIG at small $\Delta\phi$, and becomes closer to HERWIG as $\Delta\phi$ increases. The description of the measurement by CASCADE is good, whereas HERWIG is not sufficient to describe the measurement in the small $\Delta\phi$ region.

As already mentioned, the $k_\perp$-shower calculation in Figs. 5,6 depends both on unintegrated parton distributions (determined from experiment) and on $k_\perp$-dependent hard matrix elements (computed perturbatively). Fig. 7 illustrates the relative contribution of the different components of the calculation, showing different approximations to the azimuthal dijet distribution normalized to the back-to-back cross section. The solid red curve is the full result. The dashed blue curve is obtained from the same unintegrated pdf's but by taking the collinear approximation in the hard matrix element,

$$\mathcal{M}(k_\perp) \to \mathcal{M}_{collin.}(k_\perp) = \mathcal{M}(0_\perp)\ \Theta(\mu - k_\perp)\ . \tag{9}$$

The dashed curve drops much faster than the full result as $\Delta\phi$ decreases, indicating that the high-$k_\perp$component in the hard ME [9] is necessary to describe jet correlations particularly for small $\Delta\phi$. For reference we also plot, with the dotted (violet) curve, the result obtained from the unintegrated pdf without any resolved branching,

$$\mathcal{A}(x, k_\perp, \mu) \to \mathcal{A}_{no-res.}(x, k_\perp, \mu) = \mathcal{A}_0(x, k_\perp, Q_0)\ \Delta(\mu, Q_0)\quad . \tag{10}$$

Here $\mathcal{A}_0$ is the starting distribution (6) and $\Delta$ is the Sudakov form factor, giving the no-radiation probability between $Q_0$ and $\mu$. This represents the contribution of the intrinsic $k_\perp$distribution only, corresponding to nonperturbative, predominantly low-$k_\perp$modes.

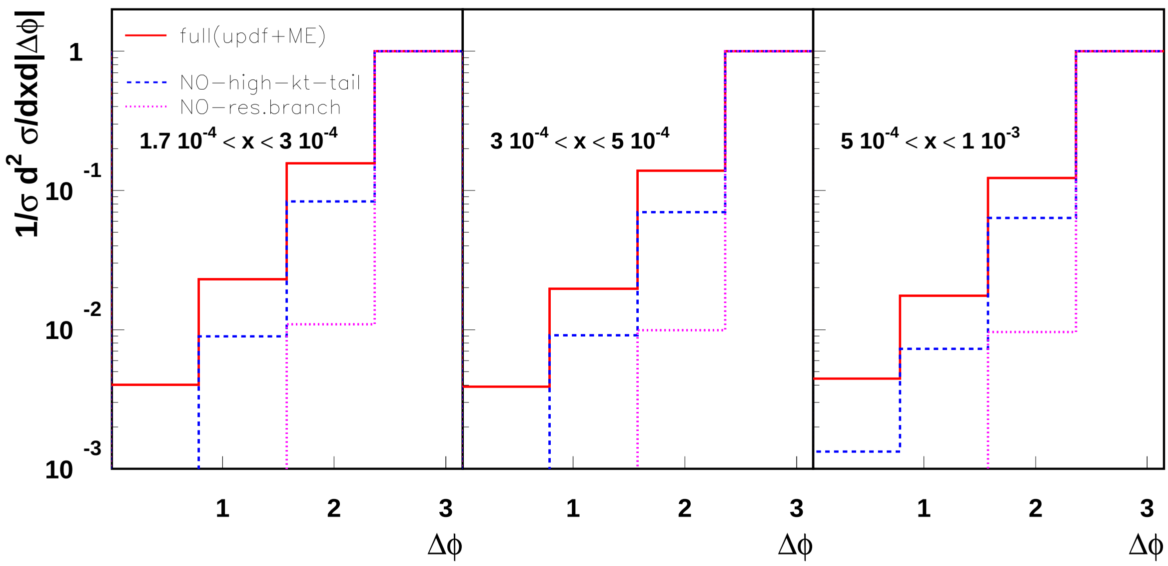


FIG. 7: Azimuthal distribution normalized to the back-to-back cross section: (solid red) full result (u-pdf $\oplus$ ME); (dashed blue) no finite-$k_\perp$correction in ME (u-pdf $\oplus$ ME$_{collin.}$); (dotted violet) u-pdf with no resolved branching.

On the whole, the results of Fig. 7 illustrate that the $k_\perp$-dependence in the unintegrated pdf alone is not sufficient to describe jet production quantitatively, and that jet correlations are sensitive to the finite, high-$k_\perp$ tail of matrix elements computed from perturbation theory.

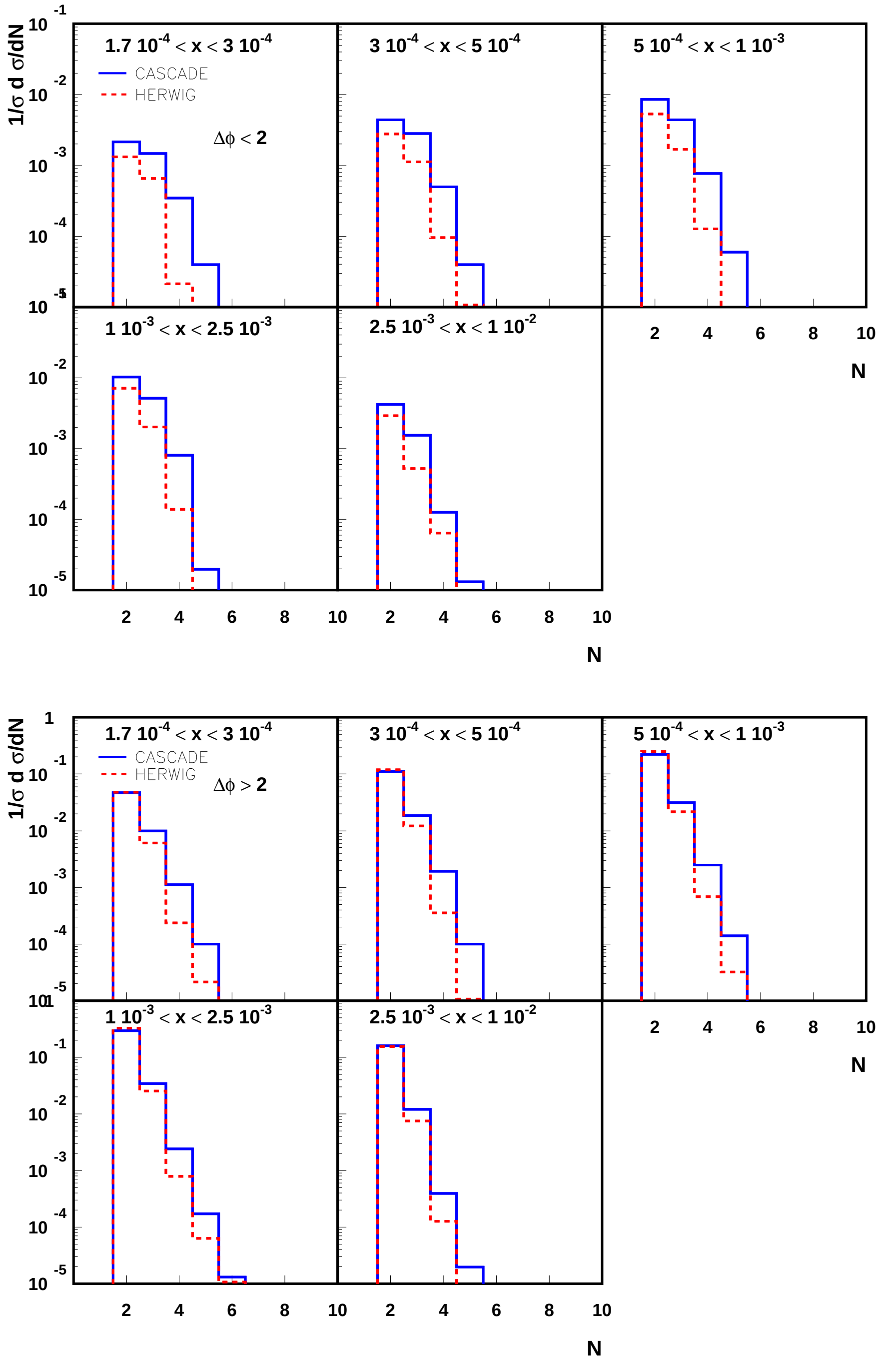


FIG. 8: Jet multiplicities obtained by CASCADE and HERWIG for (top) $\Delta\phi < 2$ and (bottom) $\Delta\phi > 2$.

Observe that the jets that we are considering are produced in the region of rapidities of Eq. (2), away from the forward region. While forward-region observables are relevant in their own right and have long been studied as probes of the initial-state shower dynamics (see e.g. [3, 35] and references therein), Monte Carlo results for such observables have a more pronounced dependence on the details of the model used for u-pdf evolution [10] (see also discussion in [17, 36]). It is thus interesting that significant effects of non-ordering in $k_\perp$ for the space-like shower are found in the present case for centrally produced hard jets.

## IV. JET MULTIPLICITIES AND MOMENTUM CORRELATIONS

We now turn to jet multiplicities and transverse-momentum correlations. These observables provide further details on the structure of the multi-jet final states. As noted in Sec. II, several of the transverse-momentum correlations measured in [15] are affected by sizeable theory uncertainties at NLO [15, 16].

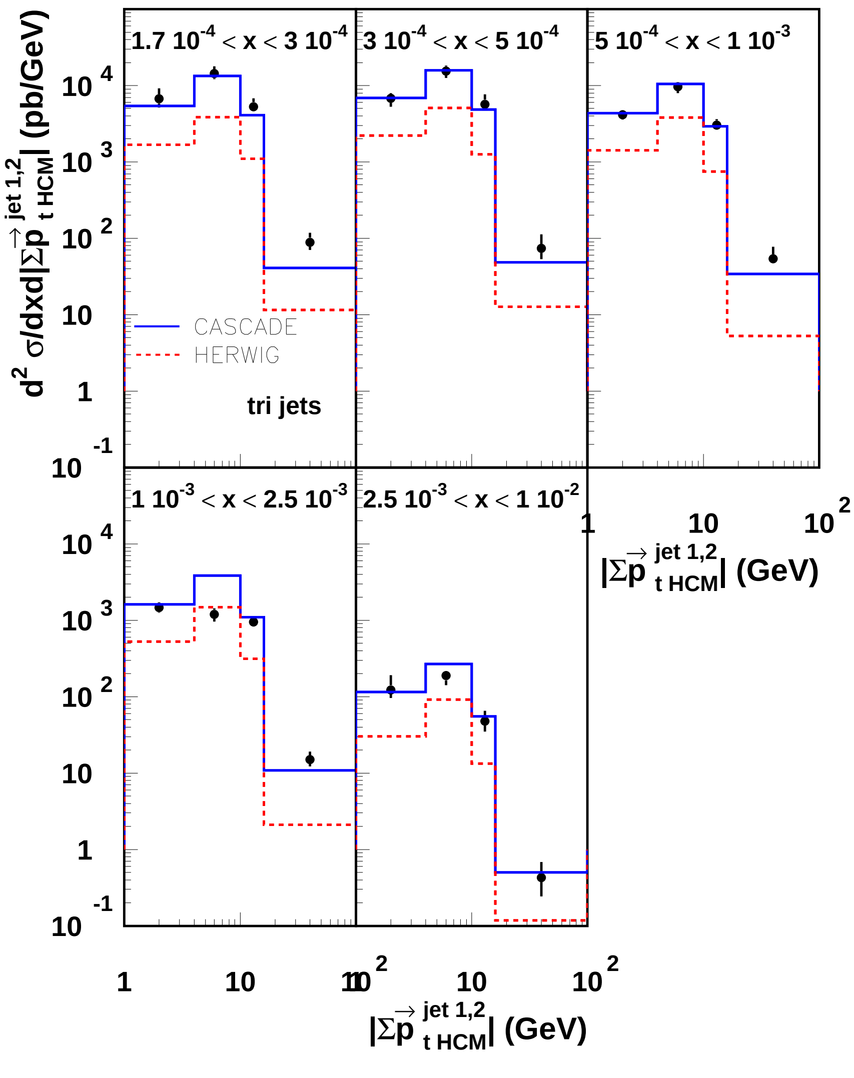


FIG. 9: Momentum correlations obtained by CASCADE and HERWIG, compared with ZEUS data [15]: three-jet cross section versus the variable $|\sum p_T^{1,2}|$ introduced in the text.

Let us first consider jet multiplicity distributions. Finite-$k_\perp$ corrections increase the mean gluon multiplicity and broaden the spectrum [7–9]. In Fig. 8 we compute the distribution in the number of jets $N$, normalized to the two-jet cross section $\sigma$, by CASCADE and HERWIG. As in Fig. 5 we show separately the results for small and large azimuthal separations between the hardest jets, $\Delta\phi < 2$ and $\Delta\phi > 2$. Jet multiplicities at small $\Delta\phi$ are where the clearest differences appear between the two parton showers. The $k_\perp$-shower result receives larger contribution from high multiplicities. Besides the absolute size of this contribution, Fig. 8 illustrates the difference in the shape between the two calculations.

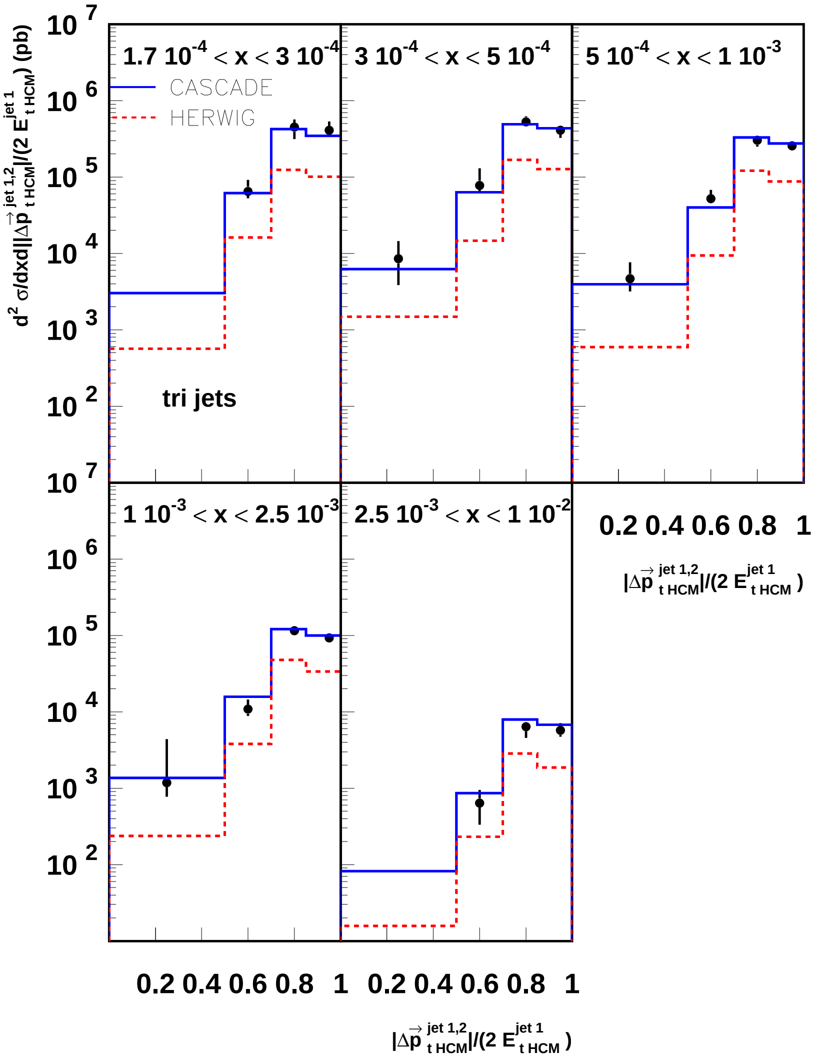


FIG. 10: Momentum correlations obtained by CASCADE and HERWIG, compared with ZEUS data [15]: three-jet cross section versus the variable $|\Delta p_T^{1,2}|/(2E_T^1)$ introduced in the text.

In Ref. [15] the ZEUS collaboration has presented measurements of various momentum correlations. We examine two such distributions for three-jet cross sections in Figs. 9 and 10, showing results of calculations by CASCADE and HERWIG along with the data [15]. In Fig. 9 is shown the distribution in the magnitude of the sum of the transverse momenta $p_T$ for the two jets with the highest $E_T$, $|\sum p_T^{1,2}|$. The back-to-back region corresponds to $|\sum p_T^{1,2}| \to 0$ in this plot. The region of large $|\sum p_T^{1,2}|$ is the region with at least three well-separated hard jets. CASCADE describes this region reasonably well. The results from HERWIG are quite lower.

In Fig. 10 is the distribution in the vector difference of the highest-$E_T$ jet transverse momenta, scaled by twice the transverse energy of the hardest jet, $|\Delta p_T^{1,2}|/(2E_T^1)$. The back-to-back region corresponds to $|\Delta p_T^{1,2}|/(2E_T^1) \to 1$ in this plot. The behavior of the Monte Carlo results compared to the data is rather similar to that in Fig. 9.

Note that the DIS kinematic region considered for the jet correlations in this section and in the previous section is characterized by the large phase space available for jet production and relatively small values of the ratio between the jet transverse momenta and center-of-mass energy. It is likely that the initial-state showering effects observed here should thus be relevant also for the understanding of distributions associated to multi-jet production at the LHC, despite the much lower energy.

## V. CONCLUSIONS

We have investigated jet correlations and associated distributions in three-jet DIS final states. For these observables next-to-leading-order results are affected by large uncertainties in the kinematic region of present data [15]. Fixed-order calculations beyond NLO are not within present reach for multi-jet processes in lepton-hadron collisions. We have studied potentially large radiative contributions at higher order by parton-shower methods complementary to those of fixed-order calculations.

We have found that including finite-$k_\perp$ radiative contributions in the initial-state shower gives sizeable effects and improves significantly the description of azimuthal correlations and transverse-momentum correlations. The differences to collinear parton shower approaches or fixed order calculations are largest in the region of small azimuthal separations between the leading jets, where the final state comprises three well-separated hard jets. The application of off-shell matrix elements convoluted with unintegrated parton distribution functions including explicit parton showering provides comparable results to NLO calculations, where applicable, and the predictions are much closer to the measurements in a region where significant higher order contributions are expected.

**Acknowledgments**. We are grateful to S. Chekanov for many discussions about the ZEUS measurements. We gratefully acknowledge many useful discussions with Z. Nagy and A. Savin. We thank the HERA machine crew and the HERA experiments for providing these precise and interesting measurements. Part of this work was done while one of us (F.H.) was visiting DESY. We thank the DESY directorate for hospitality and support.

[1] Z. Bern *et al.*, arXiv:0803.0494 [hep-ph], in Proceedings of the Workshop "Physics at TeV Colliders" (Les Houches, 2007).

[2] S. Höche, F. Krauss, N. Lavesson, L. Lönnblad, M. Mangano, A. Schälicke and S. Schumann, hep-ph/0602031; N. Lavesson and L. Lönnblad, arXiv:0712.2966 [hep-ph].

[3] S. Alekhin *et al.*, hep-ph/0601012, hep-ph/0601013: Proceedings of the Workshop "HERA and the LHC", eds. A. De Roeck and H. Jung.

[4] F. Hautmann and H. Jung, arXiv:0712.0568 [hep-ph].

[5] G. Corcella *et al.*, JHEP **0101** (2001) 010 [arXiv:hep-ph/0011363]; G. Corcella *et al.*, arXiv:hep-ph/0210213.
[6] T. Sjöstrand, S. Mrenna and P. Skands, JHEP **0605** (2006) 026.
[7] G. Marchesini and B.R. Webber, Nucl. Phys. **B386** (1992) 215.
[8] M. Ciafaloni, Nucl. Phys. **B296** (1988) 49.
[9] S. Catani, M. Ciafaloni and F. Hautmann, Phys. Lett. B **242** (1990) 97; Nucl. Phys. B**366** (1991) 135; Phys. Lett. B **307** (1993) 147.
[10] B. Andersson *et al.*, Eur. Phys. J. C **25** (2002) 77 [arXiv:hep-ph/0204115].
[11] H. Jung, Comput. Phys. Commun. **143** (2002) 100 [arXiv:hep-ph/0109102]; H. Jung and G.P. Salam, Eur. Phys. J. C **19** (2001) 351 [arXiv:hep-ph/0012143].
[12] L. Lönnblad and M. Sjödahl, JHEP **0505** (2005) 038; JHEP **0402** (2004) 042; G. Gustafson, L. Lönnblad and G. Miu, JHEP **0209** (2002) 005.
[13] K. Golec-Biernat, S. Jadach, W. Placzek, P. Stephens and M. Skrzypek, hep-ph/0703317.
[14] S. Höche, F. Krauss and T. Teubner, arXiv:0705.4577 [hep-ph].
[15] S. Chekanov *et al.* [ZEUS Collaboration], Nucl. Phys. B **786** (2007) 152 [arXiv:0705.1931 [hep-ex]].
[16] Z. Nagy and Z. Trocsanyi, Phys. Rev. Lett. **87** (2001) 082001 [arXiv:hep-ph/0104315].
[17] J.C. Collins, T.C. Rogers and A.M. Stasto, arXiv:0708.2833 [hep-ph].
[18] F. Hautmann, Phys. Lett. B **655** (2007) 26 [arXiv:hep-ph/0702196].
[19] J.R. Forshaw, A. Kyrieleis and M.H. Seymour, JHEP **0608** (2006) 059.
[20] J.C. Collins, arXiv:0708.4410 [hep-ph]; W. Vogelsang and F. Yuan, Phys. Rev. D **76** (2007) 094013; C.J. Bomhof and P.J. Mulders, Nucl. Phys. B**795** (2008) 409.
[21] A. Bacchetta, D. Boer, M. Diehl and P.J. Mulders, arXiv:0803.0227 [hep-ph].
[22] I.O. Cherednikov and N.G. Stefanis, arXiv:0802.2821 [hep-ph].
[23] C.W. Bauer, F.J. Tackmann and J. Thaler, arXiv:0801.4028; arXiv:0801.4026.
[24] J.C. Collins and F. Hautmann, JHEP **0103** (2001) 016; Phys. Lett. B **472** (2000) 129.
[25] F. Hautmann, arXiv:0708.1319 [hep-ph].
[26] F. Hautmann and H. Jung, arXiv:0804.1746 [hep-ph], in Proceedings of the 8th International Symposium on Radiative Corrections RADCOR2007 (Florence, October 2007).
[27] A. Aktas *et al.* [H1 Collaboration], Eur. Phys. J. C **33** (2004) 477 [arXiv:hep-ex/0310019].
[28] M. Hansson [H1 Collaboration], in Proceedings of the 14th International Workshop on Deep Inelastic Scattering DIS2006 (Tsukuba, April 2006), p. 539.
[29] C. Adloff *et al.* [H1 Collaboration], Eur. Phys. J. C **19** (2001) 269 [arXiv:hep-ex/0012052].
[30] Y. Delenda, R. Appleby, M. Dasgupta and A. Banfi, JHEP **0612** (2006) 044 [arXiv:hep-ph/0610242].
[31] A. Banfi and M. Dasgupta, JHEP **0401** (2004) 027.
[32] Y. Delenda, arXiv:0706.2172; A. Banfi, M. Dasgupta and Y. Delenda, arXiv:0804.3786.
[33] H. Jung, Mod. Phys. Lett. A**19** (2004) 1.
[34] M. Hansson and H. Jung, arXiv:0707.4276 [hep-ph].
[35] J.R. Andersen *et al.*, Eur. Phys. J. C **35** (2004) 67.
[36] J.C. Collins, hep-ph/0106126, in Proceedings of the Workshop DIS01 (Bologna, 2001).